Multiphoton ionization of lead monofluoride resonantly enhanced by the $X_1\,^2\Pi_{1/2} \rightarrow B\,^2\Sigma_{1/2}$ transition

C. P. McRaven, P. Sivakumar, and N. E. Shafer-Ray*
The University of Oklahoma, 440 West Brooks Street, Norman, Oklahoma 73019, USA
(Received 5 December 2006; published 28 February 2007)

Resonance enhanced multiphoton ionization of the $X_1\,^2\Pi_{1/2}$ state of lead monofluoride ($^{208}Pb^{19}F$) via the $B\,^2\Sigma_{1/2}$ state is demonstrated. The ionization potential is observed to be 7.54(1) eV. Limits on the lifetime of the B state are found to be consistent with that reported by Chen *et al.* The transition dipole moment for the $X_1 \rightarrow B$ transition is found to be 0.005(1) a.u. Limits on the ionization cross section of the B state are found.

DOI: 10.1103/PhysRevA.75.024502 PACS number(s): 33.15.Ry, 33.70.Ca, 33.80.Rv

I. INTRODUCTION

The stationary states of a particle in a pure electric field exhibit a degeneracy in the sign of the projection m_F of total angular momentum on the electric field. Verification of this degeneracy to ~ 60 μHz for the $^2P_{1/2}$, $F=1$, $m_F=\pm 1$ ground state of Tl atoms in a 123 kV/cm (typical) electric field is responsible for the current limit on the electron-electric dipole moment (e-EDM) [1]. This limit places important constraints on fundamental theories of particles and interactions [2], and has already entered the regime of allowable values for the e-EDM put forth by Supersymmetry (10^{-30} e cm $< d_{e,\mathrm{SUSY}} < 10^{-25}$ e cm) [3]. Heavy paramagnetic molecules have been proposed to be especially sensitive to the e-EDM [4]. In particular, the molecules HgF, YbF, and PbF have been shown to offer a factor of 1000 improvement in sensitivity to the e-EDM over atoms [5,6]. We have suggested that $^{208}Pb^{19}F$ has the additional advantage that in a strong electric field the magnetic g factor becomes very small, suppressing systematic errors due to background magnetic fields [7]. This advantage motivates the study of resonance enhanced multiphoton ionization (REMPI) of PbF presented here.

Whereas gas-phase YbF and PbF have been detected by laser induced fluorescence [6,8,9], and matrix-isolated HgF has been detected by electron spin resonance [10], this work is the first demonstration of REMPI for any of these e-EDM sensitive molecules. The next section describes our experimental apparatus. Section III presents our measurement of the ionization potential of PbF, our determination of the limits on the lifetime of the B state, our measurement of the mean transition dipole moment of the $X_1 \rightarrow B$ transition, and our determination of the limits on the ionization cross section of the B state. Section IV presents conclusions.

II. EXPERIMENTAL

A molecular beam of PbF molecules is created using an effusive nozzle constructed from MgF_2. This nozzle is designed with a small reservoir to contain molten lead near its 0.2-mm-diam exit orifice. The nozzle is radiatively heated to 1100–1200 K. At these temperatures, the lead reacts with the MgF_2 walls of the cell to form PbF molecules. Helium gas enters the back of the nozzle, passes over the molten lead, and exits through the orifice carrying the PbF product with it. This PbF enters a vacuum chamber, passes through a skimmer, and finally enters a differentially pumped high vacuum chamber.

Linearly polarized laser radiation ionizes the PbF. This ionizing laser radiation is produced by two independent 10 ns, pulsed Nd:YAG-pumped dye laser systems (Quanta Ray GCR-pumped Lambda Physik Scanmate 2E, Continuum Shurlite-pumped Lambda Physik Scanmate 2E). The first laser system (the pump laser) produces laser radiation at 280 nm to excite the $X_1\,^2\Pi_{1/2} \rightarrow B\,^2\Sigma_{1/2}$ transition. The second laser system (the probe laser) produces laser radiation at 395 nm to ionize the B state. The polarization of both the 280 and 395 nm laser radiation is perpendicular to the molecular beam. Both sources of laser radiation propagate together, are cylindrically focused, and cross at a right angle to the molecular beam. The ionized PbF is detected using a time-of-flight mass spectrometer described previously [11]. A typical mass spectrum is shown in the inset of Fig. 1. All measurements, including the spectra shown in Fig. 1, are made while gating on the $^{208}Pb^{19}F$ peak of the mass spectrum.

III. DISCUSSION

This section describes the measurement of the ionization potential, the determination of the limits on the lifetime of

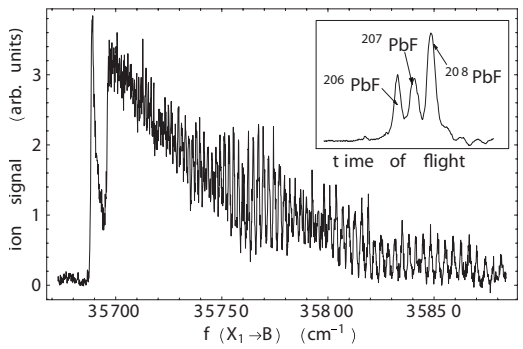

FIG. 1. Spectrum of the $X_1 \rightarrow B$ transition of PbF. A typical mass time-of-flight spectra is shown in the inset.

*Author to whom correspondence should be addressed.

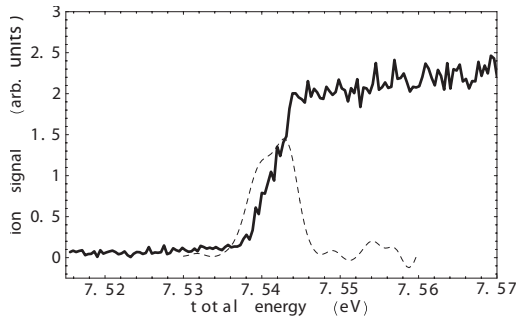

FIG. 2. Appearance potential of PbF ions with the derivative of smoothed data (dashed line).

the B state, the measurement of the transition dipole moment of the $X_1 \rightarrow B$ transition, and the determination of the limits on the ionization cross section of the B state. The ionization energy is measured by tuning the pump laser radiation to the bandhead of the $X_1 \rightarrow B$ transition (35 689 cm^{-1}) and scanning the wavelength of the probe laser radiation. The appearance potential of ions is shown in Fig. 2. To confirm that this appearance does not correspond to the production of a vibrationally excited ion, the probe laser is scanned 1800 cm^{-1} to the red, and no ions are observed. We conclude that this appearance potential corresponds to the ionization threshold of PbF. To determine the ionization potential from the data of Fig. 2, the data are smoothed and differentiated. The resulting peak is shown by the dashed line in Fig. 2. The centroid of the peak is taken as the ionization potential. Systematic effects that could shift this centroid include pulsed-field ionization of Rydberg states by the extraction field of our mass spectrometer and a difference, $\Delta\beta$, between the rotational constants of the B state and the PbF^+ ion. To estimate the former systematic effect, the Rydberg-type structure is observed for a single rotational line at high J. The width of this structure before the onset of continuous ionization is similar to the width of the differentiation peak. The latter systematic effect is estimated by $\Delta\beta J^2$ with $J \approx 20.5$, corresponding to the turning point of the bandhead, and $\Delta\beta \approx 0.1$, half the rotational constant of the ground state. This estimate gives a shift of 0.0065 eV, also comparable to the width of the differentiation peak. Because both systematic errors are comparable to the 0.007 eV width of the differentiation peak, we take our uncertainty to be 0.01 eV. A comparison of our experimental ionization potential for $^{208}Pb^{19}F$ to other group IV A monofluorides is given in Table I.

TABLE I. Comparison of ionization energies of other group IV A monofluorides.

Molecule	Ionization energy (eV)	Source
SiF	7.31(2)	Ref. [12]
GeF	7.28	Ref. [13]
SnF	7.3(3)	Ref. [14]
PbF	7.5(3)	Ref. [14]
$^{208}Pb^{19}F$	7.54(1)	This work

The dependence of the ion signal on pump-probe delay time shows no indication of ionization without temporal overlap of the pump and probe laser radiation. We conclude that the lifetime is less than 2 ns, consistent with the observation of Chen *et al.* [8]. The dependence of the ion signal of an isolated transition at high J ($\sim$73.5) on the pump laser radiation frequency gives a full width at half maximum (FWHM) linewidth $\Delta\nu_{\mathrm{FWHM}}$ of 1 cm^{-1}. However, we are unable to determine whether the linewidth is due to the physical lifetime of the B state or an artifact of the modal structure of our unseeded Nd:YAG laser. The combined observation of time-delayed ionization and linewidth only allows us to place loose limits on the rate of decay of the B state k_d,

$$0.03 \text{ ns} < \frac{1}{k_d} < 2 \text{ ns}. \tag{1}$$

Along with the measurement of the linewidth of an isolated rotational line, we observe and model the dependence of the ion signal on the peak intensity of the pump and probe lasers as shown in Fig. 3. (Here we define peak intensity to correspond to the condition of a Gaussian-time profile, ignoring the detailed temporal structure of the laser radiation.) The assumed kinetic model for excitation and ionization is shown in Fig. 4. The model includes populations of the X_1 state, B state, an ionization state, and a decay state. This decay state models the decay of the B state to a multitude of states in-

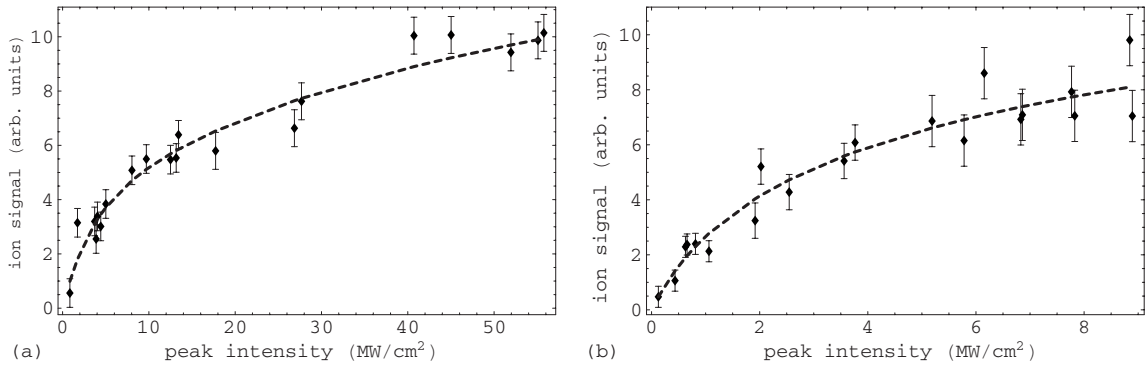

FIG. 3. Observed (points) and modeled (dashed lines) dependence of ionization signal on peak intensities of the laser radiation. (a) Dependence on pump ($X_1 \rightarrow B$) intensity with probe (ionization) intensity at 9.5 MW/cm^2. (b) Dependence on probe (ionization) intensity with pump ($X_1 \rightarrow B$) intensity at less than 1 MW/cm^2.

$$[X_1] \overset{k_b}{\rightleftharpoons} [B] \overset{k_+}{\rightharpoonup} [+]$$
$$\downarrow k_d$$
$$[d]$$

FIG. 4. Representation of the differential equations used to simulate the saturation.

accessible by ionization laser radiation. The rates of population transfer between these states are given by k_b, k_+, and k_d.

Applying Fermi's golden rule, the rate constant k_b is related to the mean transition dipole moment for excitation by linear polarized light d_b, by

$$k_b = 16\pi^2 \alpha N \left(\frac{d_b}{e}\right)^2 \frac{I_b}{h\Delta\nu_{\mathrm{FWHM}}} e^{-4\ln 2(t^2/\Delta t^2 + x^2/\Delta x^2 + y^2/\Delta y^2)}. \tag{2}$$

Here α is the fine structure constant, e is the electron charge, h is Planck's constant, I_b is the peak intensity of the 280 nm $X_1 \rightarrow B$ laser radiation, N is given by $N=\sqrt{4\ln 2/\pi}$, and Δt, Δx, and Δy are experimentally determined to be 7 ns, 30 μm, and 3000 μm, respectively. The ionization rate k_+ is related to the ionization cross section σ_{ion} by

$$k_+ = \sigma_{\mathrm{ion}} \frac{I_+}{h\nu} e^{-4\ln 2(t^2/\Delta t^2 + x^2/\Delta x^2 + y^2/\Delta y^2)}. \tag{3}$$

Here I_+ is the peak intensity of the 395 nm ionization laser radiation. To create our model of ion signal intensity as a function of I_b and I_+, the rate equations resulting from Fig. 4 and Eqs. (2) and (3) are integrated over time and the resulting yield of the ion state is integrated over the x-y spatial coordinates.

The best fits to the data are shown as dashed lines in Fig. 3. At the least intense values of laser radiation both the pump and probe steps show linear behavior. As the laser intensity increases, saturation effects are observed. The gradual increase in ion signal intensity at the strongest laser intensities is due to the increased efficiency of ionization in the wings of the focused beam waist. This change of curvature from linear to saturation behavior allows for sensitivity to transition strengths without making the difficult measurement of absolute ionization yield. The best fit to the dependence of the $X_1 \rightarrow B$ transition on peak intensity gives a transition dipole moment of 0.005(1) a.u. The error in the best fit is taken to be the standard deviation of the distribution of the fits to the pump laser intensity dependence as it is the dominant contribution of error. As ionization and decay are competing processes, the parameters σ_{ion} and k_d are strongly correlated. We find our data are only sensitive to their ratio with

$$\sigma_{\mathrm{ion}} = \sigma_0 k_d \tau_{\mathrm{FWHM}}, \tag{4}$$

where σ_0=22(8) Gb and τ_{FWHM}=0.03 ns. The error in σ_0 is taken to be the standard deviation of the distribution of the fits to the probe laser intensity dependence. Using the limits on the lifetime in Eq. (1), the loose limits on the ionization cross section are 22 Gb $> \sigma_{\mathrm{ion}} >$ 0.33 Gb.

IV. CONCLUSION

Multiphoton ionization of PbF has been achieved via the B state. The transition dipole moment of the $X_1 \rightarrow B$ transition is found to be 0.005(1) a.u. The ionization potential is found to be 7.54(1) eV. Loose limits on both the lifetime (0.03 ns $< 1/k_d <$ 2 ns) and the ionization cross section (22 Gb $> \sigma_{\mathrm{ion}} >$ 33 Gb) of the B state have been determined. These values may provide benchmarks for expanding work in electronic structure calculations [15]. Our findings present mixed news for the use of $X_1 \rightarrow B$ REMPI for the detection of PbF. Whereas the transition dipole moment, ionization cross section, and ionization potential allow for ionization of PbF at convenient operating wavelengths and power, the short lifetime of the B state is unlikely to allow for the resolution of low-J rotational states.

ACKNOWLEDGMENTS

The authors are thankful to the National Science Foundation (PHY-0602490) for its support of this research.

[1] B. C. Regan, Eugene D. Commins, Christian J. Schmidt, and David DeMille, Phys. Rev. Lett. **88**, 071805 (2002).
[2] I. B. Khriplovich and S. K. Lamoreaux, *CP Violation Without Strangeness: Electric Dipole Moments of Particles, Atoms, and Molecules* (Springer-Verlag, Berlin, 1997).
[3] R. Arnowitt, B. Dutta, and Y. Santoso, Phys. Rev. D **64**, 113010 (2001).
[4] P. Sandars, At. Phys. **4**, 71 (1975).
[5] M. G. Kozlov and L. N. Labzowsky, J. Phys. B **28**, 1933 (1995).
[6] J. J. Hudson, B. E. Sauer, M. R. Tarbutt, and E. A. Hinds, Phys. Rev. Lett. **89**, 023003 (2002).
[7] N. E. Shafer-Ray, Phys. Rev. A **73**, 034102 (2006).
[8] Jing Chen and Paul J. Dagdigian, J. Chem. Phys. **96**, 1030 (1992).
[9] O. Shestakov, A. M. Pravilov, H. Demes, and E. H. Fink, Chem. Phys. **165**, 415 (1992).
[10] L. B. Knight, T. A. Fisher, and M. B. Wise, J. Chem. Phys. **74**, 6009 (1981).
[11] Chris McRaven, Janis Alnis, Brendan Furneaux, and Neil Shafer-Ray, J. Phys. Chem. A **107**, 7138 (2003).
[12] H. Bredohl, J. Breton, I. Dubois, J. M. Esteva, D. Macau-Hercot, and F. Remy, J. Mol. Spectrosc. **195**, 281 (1999).
[13] J. W. C. Johns and R. F. Barrow, Proc. Phys. Soc. London **71**, 476 (1958).
[14] K. Zmbov, J. W. Hastie, and J. L. Margrave, Trans. Faraday Soc. **64**, 861 (1968).
[15] K. Balasubramanian, J. Chem. Phys. **83**, 2311 (1985).